Original Article

A predictive model based on radiomics, clinical features, and pathologic indicators for disease-free survival after liver transplantation for hepatocellular carcinoma: a 7-year retrospective study

Hao Xie[1,2], Bin Shi[3], Junzhen Fan[4], Shui Liu[5], Qiaozhi Ma[6], Junnan Dai[6], Siqing Dong[7], Ying Liu[8], Han Meng[1], Hui Liu[2], Ya Yang[9], Xuetao Mu[6]

[1]Postgraduate Training Base of the Third Medical Center of Chinese PLA General Hospital, Jinzhou Medical University, Beijing, China; [2]Department of Radiology, the Jintang First People's Hospital, Chengdu, China; [3]Department of Organ Transplantation, the Third Medical Center of Chinese PLA General Hospital, Beijing, China; [4]Department of Pathology, the Third Medical Center of Chinese PLA General Hospital, Beijing, China; [5]Department of Radiology, Aerospace Center Hospital, Beijing, China; [6]Department of Radiology, the Third Medical Center of Chinese PLA General Hospital, Beijing, China; [7]Department of Radiation Oncology, Jinzhou Central Hospital, Jinzhou, China; [8]School of Medical Imaging, Weifang Medical University, Weifang, China; [9]Department of Ultrasound Medicine, the Jintang First People's Hospital, Chengdu, China

Contributions: (I) Conception and design: X Mu, B Shi, H Xie, J Fan, S Liu; (II) Administrative support: X Mu, B Shi, J Fan; (III) Provision of study materials or patients: B Shi, H Xie, Q Ma; (IV) Collection and assembly of data: B Shi, H Xie, J Fan, Q Ma, J Dai, S Dong, Y Liu, H Meng; (V) Data analysis and interpretation: H Xie, J Fan, S Liu, J Dai, S Dong, H Liu, Y Yang; (VI) Manuscript writing: All authors; (VII) Final approval of manuscript: All authors.

Correspondence to: Xuetao Mu, MD. Department of Radiology, the Third Medical Center of Chinese PLA General Hospital, No. 69, Yongding Road, Haidian District, Beijing 100039, China. Email: 2464878078@qq.com.

Background: Disease-free survival (DFS) is an essential indicator for evaluating the prognosis of liver transplantation (LT) in hepatocellular carcinoma (HCC) patients. Despite progress in the prediction of DFS by radiomics, only preoperative clinical features have been combined in most studies. The aim of this study was to construct a nomogram model (NM) using preoperative clinical features, radiomics, and postoperative pathological indicators for more effective prediction of DFS.

Methods: This was a retrospective study of a single-center cohort comprising 139 HCC patients. Using the whole cohort, we constructed and assessed a clinical model (CM) based on alpha-fetoprotein (AFP) and alkaline phosphatase (ALP), a pathological model (PM) based on Ki-67 and tumor number, a radiomics model (RM) based on the radiomics score (Rad-score), and an NM based on the above five independent predictors.

Results: Significant correlations between the NM and DFS were observed in the training and validation cohorts. Among the four prediction models, the C-index of the NM was the highest [(training/validation cohort) CM: 0.664/0.676, PM: 0.737/0.691, RM: 0.706/0.697, NM: 0.817/0.760], and the areas under the receiver operating characteristic curves (AUCs) of the NM prediction of 1-year, 2-year, and 3-year DFS were also the highest [(training/validation cohort) 1-year, 2-year, and 3-year CM: 0.726/0.726, 0.685/0.744, 0.645/0.686, PM: 0.789/0.780, 0.801/0.748, 0.841/0.735, RM: 0.769/0.752, 0.717/0.805, 0.748/0.765, NM: 0.882/0.854, 0.867/0.849, 0.882/0.801]. The NM also exhibited the highest net clinical benefit.

Conclusions: Based on radiomics, clinical features, and pathological indicators, the NM could be used to effectively predict DFS after LT in HCC patients, guiding the follow-up and complementary treatment.

Keywords: Hepatocellular carcinoma (HCC); liver transplantation (LT); nomogram model (NM); radiomics; disease-free survival (DFS)

Submitted May 11, 2024. Accepted for publication Sep 04, 2024. Published online Oct 29, 2024.
doi: 10.21037/jgo-24-347
View this article at: https://dx.doi.org/10.21037/jgo-24-347

Introduction

Primary hepatocellular carcinoma (PHC) is the sixth most common malignancy in the world, the third leading cause of cancer-related deaths, and the second leading cause of cancer-specific deaths in the Asia-Pacific region, particularly in China (1,2). Hepatocellular carcinoma (HCC) accounts for 75–85% of PHCs (3). The incidence of HCC is on the rise globally, especially in recent years, with more than 50% of new cases found in China (4). Several large-scale clinical investigations have indicated that the peak recurrence of HCC occurs within 2–3 years following transplantation even though liver transplantation (LT) is one of the most effective therapies for HCC (5). Furthermore, recurrence of HCC within 1 year of transplantation is considered early recurrence and indicates a poor prognosis for patients (6). Many factors influence the prognosis of HCC patients after LT; therefore, early prediction of patients' disease-free survival (DFS) is crucial for long-term care and effective treatment (7).

Alpha-fetoprotein (AFP) is frequently used to diagnose HCC, track treatment response, evaluate prognosis, and identify early recurrences (8). The specificity of AFP in diagnosing HCC is 99–100%, but the sensitivity is only 20–45% (8). In addition, nearly 30% of HCC patients also express negative AFP levels (9). Therefore, the use of AFP alone as a biomarker for predicting prognosis in HCC still has limitations. Alkaline phosphatase (ALP) is also found to be significantly associated with a worse prognosis in individuals with HCC (10).

The pathologic immunohistochemical marker Ki-67, a nuclear antigen associated with cell proliferative activity, is a commonly used indicator of the level of cell proliferation and is positively correlated with tumor aggressiveness (11). In many studies, scholars have successfully predicted the presence of Ki-67 in numerous malignant tumors, including lung cancer (12) and breast cancer (13). Recent research has shown that Ki-67 is the most valuable independent predictor for assessing early recurrence and a poor prognosis in surgically resected HCC (14) and that patients with HCC who express high levels of Ki-67 have lower overall survival (OS) (15) and DFS (16).

Conventional imaging studies are based on tumor shape, density, and enhancement (17) without quantifying the image information, making them susceptible to the subjectivity of radiologists and ignoring intratumoral heterogeneity (ITH) (18). On the other hand, radiomics is a quantitative feature extraction technique with high throughput that transforms images into data that can be mined. Several investigations have demonstrated that radiomics features, which offer far more predictive information than clinical features, correspond with the biological properties of malignancies (7). Radiomics has been shown to provide new perspectives for precision medicine in oncology practice, correlating with DFS (16), metastasis prediction (19), and treatment response assessment (20).

Nevertheless, many limitations exist when relying solely on radiomics, clinical features, and pathologic indicators. For instance, approximately 30% of HCC patients may have AFP negativity (9); Ki-67 only reacts to proliferation within the tumor, and there are different definitions of high expression in different tumors for which no clear standard exists. Furthermore, most of the existing radiomics only

Highlight box

Key findings

- The study developed and validated a nomogram model (NM) constructed from radiomics, clinical features, and pathological indicators to predict disease-free survival after liver transplantation in hepatocellular carcinoma (HCC) patients.

What is known and what is new?

- In previous studies, radiomics has been used to predict the prognosis of HCC patients, and radiomics has been used to predict postoperative Ki-67 expression in HCC patients.
- This study fully utilized the preoperative clinical features, preoperative computed tomography radiomics, and postoperative pathological indicators of patients to develop and validate a more precise NM that could guide adjuvant treatment and follow-up after liver transplantation and predict disease-free survival in HCC patients.

What is the implication, and what should change now?

- The NM constructed in this study could predict the prognosis of HCC patients after liver transplantation. Of course, external validation of the model, as well as further incorporation of genomics for better predictive ability, will be needed in the future.

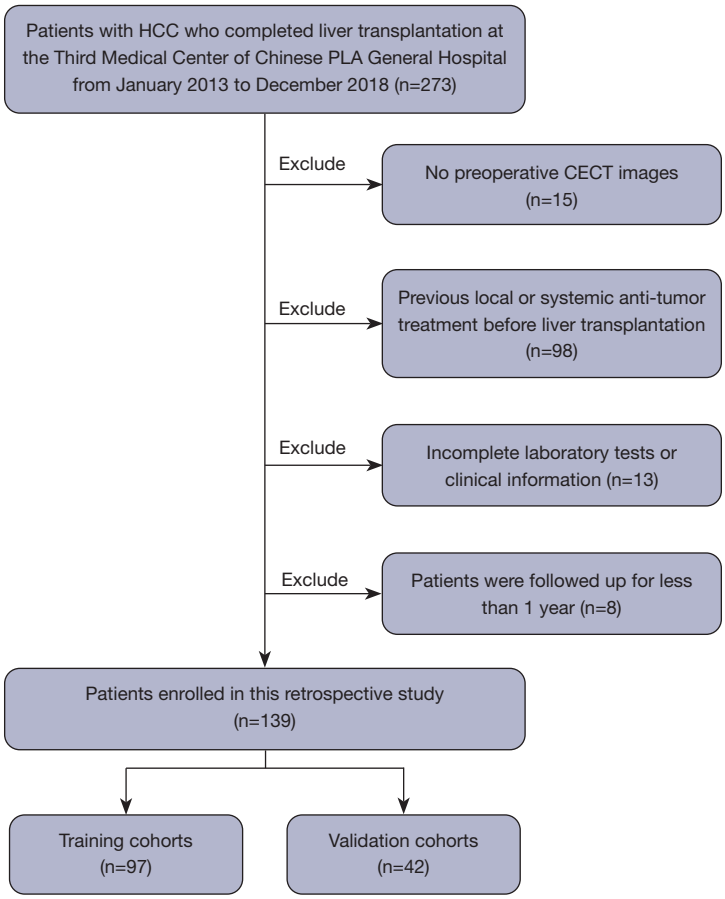

Figure 1 Inclusion and exclusion flowchart. HCC, hepatocellular carcinoma; CECT, contrast-enhanced computed tomography.

focus on ITH and microvascular invasion (MVI). Therefore, the prediction of DFS in patients with HCC may be more accurate if the above features can all be included to create a prediction model.

In this study, we aimed to develop and validate a nomogram model (NM) constructed from radiomics, clinical features, and pathological indicators to predict DFS after LT in HCC patients. This model could be used to inform the follow-up and complementary treatment. We present this article in accordance with the TRIPOD reporting checklist (available at https://jgo.amegroups.com/article/view/10.21037/jgo-24-347/rc).

Methods

Study population

The study was conducted in accordance with the Declaration of Helsinki (as revised in 2013). The study was approved by the Medical Ethics Review Committee of the Third Medical Center of Chinese People's Liberation Army (PLA) General Hospital (No. KY2024-016) and individual consent for this retrospective analysis was waived. Between January 2013 and December 2018, a total of 273 patients with HCC from the Third Medical Center of Chinese PLA General Hospital were treated with LT. Based on the inclusion and exclusion criteria, the enrolled patients were randomized into a training cohort and a validation cohort at a ratio of 7:3. The inclusion criteria were (I) regular follow-up after LT and (II) HCC confirmed by pathophysiology. The exclusion criteria were as follows: (I) patients without preoperative contrast-enhanced computed tomography (CECT) images; (II) patients who had received other systemic or local anti-tumor treatments before LT; (III) patients with incomplete laboratory tests, demographic data, and follow-up information; and (IV) patients with less than 1 year of follow-up. *Figure 1* shows the inclusion and exclusion process.

Follow-up

During the follow-up period, liver function tests, ultrasonography, abdominal computed tomography (CT) or magnetic resonance imaging (MRI) scans, and other necessary laboratory tests, such as AFP, were performed on the patients 1 month after LT and every 3 months thereafter; furthermore, the patients were continuously followed up for at least 1 year from the date of the LT procedure until recurrence, with a follow-up cutoff point of January 1, 2020. HCC recurrence after LT was considered detected when there were typical imaging manifestations, laboratory indicators, or pathologic indicators of intrahepatic recurrence or extrahepatic metastasis.

DFS was the primary endpoint of this study, indicating the period of time between detection of HCC recurrence and LT.

CECT image acquisition

Multiphase dynamic CECT of the liver was performed on the patient using a 64-row CT device (Discovery CT750 HD, GE Healthcare), referring to the two modalities arterial phase (AP) and venous phase (VP). A plain scan was performed first, and then a contrast agent (Omnipaque 320, GE Healthcare) was injected through the median elbow vein at a rate of 3.0 mL/s. An AP scan was performed with a delay of 25 s, a VP scan was performed 30 s after the end of the AP scan, and the AP- and VP-CECT images were obtained. Sensitive information was removed, and all images were anonymized and stored in DICOM format. The CT scan parameters are shown in Table S1.

Collection of clinical features and pathological indicators

Preoperative clinical data of each HCC patient were collected through the hospital information management system, including demographic characteristics (age, sex), liver function Child rating characteristics, and laboratory tests [hepatitis B surface antigen (HBsAg), AFP, and ALP]. The postoperative pathological data, such as Ki-67 expression, tumor number, and maximum tumor diameter, were also collected. Ki-67 was the percentage of positive cells to the total cells, and the average value was taken, which was categorized as low Ki-67 expression (<10%) or high Ki-67 expression (≥10%) according to previous studies (16,21).

Radiomics analysis and radiomics model (RM) development

3D-Slicer software (version 4.8.1 r26813) was used for tumor segmentation, and manual outlining was used to define a region of interest (ROI) on each layer of the tumor display. In the case of multiple tumors on the liver, only the ROIs of the largest of them were outlined. Intra- and intergroup correlation coefficients (ICCs) were used to assess the repeatability of the imaging histology characteristics. A randomly selected batch of 30 patients' lesions was outlined by radiologist 1 and radiologist 2; the same procedure was repeated by radiologist 1 two weeks later. Radiomics features with both ICCs >0.75 were taken as standards for good reproducibility. Finally, the tumor ROIs of the remaining patients were manually outlined by radiologist 1.

Radiomics features for each patient were extracted from AP- and VP-CECT images using the Python software PyRadiomics package (version 3.0.3) and were classified into the following seven categories: first-order statistic; shape features (3D); gray-level cooccurrence matrix (GLCM); gray-level size zone matrix (GLSZM); gray-level run-length matrix (GLRLM); neighborhood gray-tone difference matrix (NGTDM); gray-level dependence matrix (GLDM). In addition, a tiny filter was applied to the original image to obtain a derived image for each patient. The original and derived images were used to compute all feature classes except form features. Due to the large number of extracted radiomics features, dimensionality reduction was necessary for removing redundant features, obtaining essential features, and realizing data visualization. First, radiomics features with ICCs >0.75 were correlated using Spearman's rank correlation test to remove redundant features with linear correlation coefficients >0.9; then the logistic regression (LR) model was used to identify the most valuable features; finally, the selected radiomics features and their weighting coefficients were linearly combined to generate a radiomics score (Rad-score).

Additionally, using the median Rad-score from the training cohort as the threshold value, we assigned the patients to high-risk and low-risk groups. Kaplan-Meier survival analysis (*Figure 2A*,*2B*) was used to determine

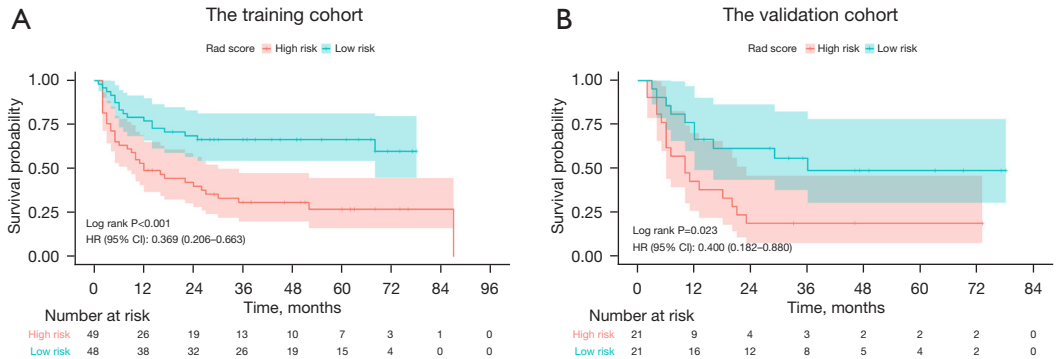

Figure 2 Estimated DFS of HCC patients after LT by Rad-score (A,B). DFS, disease-free survival; HCC, hepatocellular carcinoma; LT, liver transplantation; Rad-score, radiomics score; HR, hazard ratio; CI, confidence interval.

the correlation between the Rad-score and DFS, and this information was used to construct a RM.

Predictive model development and performance comparison

COX survival unifactorial and multifactorial analyses of clinical features, pathological indicators, and Rad-scores were performed to obtain independent predictors associated with postoperative DFS of LT and to construct a clinical model (CM), a pathological model (PM), and an NM, respectively. The area under the receiver operating characteristic curve (AUC), Harrell's concordance index (C-index), and decision curve analysis (DCA) were used to assess and compare the performance of the four prediction models with the clinical benefit performance. Calibration curves were used to assess the consistency of the NM's prognostic performance in the training and validation cohorts. Kaplan-Meier survival analysis was used to assess the risk stratification ability of the NM.

Statistical analysis

Distribution normality was tested using the Shapiro-Wilk test. Clinical features and pathological indicators were compared using Student's *t*-test. Continuous variables conforming to a normal distribution were expressed as the mean ± standard deviation. Continuous variables that were not normally distributed were compared using the Wilcoxon signed rank test and expressed as the median of the interquartile range. Categorical variables were compared using the Pearson χ^2 test. Correlation analysis was performed using the Spearman rank correlation test to remove redundant features. Kaplan-Meier survival analysis was used to compare the different survival rates of the low-risk and high-risk groups. Cox survival analysis was used to determine the independent predictors for constructing nomograms. The rms and regplot packages were used to build nomograms and calibration curves. The dcurves package was used to build DCA curves. The pec package was employed to calculate the C-index. The receiver operating characteristic curve (ROC) package was used for ROC curve analysis. All statistical analyses were performed using SPSS software (version 24.0) or R software (version 4.1.2), and P<0.05 was considered statistically significant.

Results

Clinical characteristics and pathological indicators

A total of 139 patients who finally met the requirements for enrollment were randomized into a training cohort (n=97) and a validation cohort (n=42) at a 7:3 ratio. The clinical and pathological characteristics of the two groups are compared in *Table 1*. The difference in the baseline characteristics of the two cohorts was not statistically significant (P>0.05).

RM development

A total of 1,702 features were extracted from AP- and VP-CECT images, and the five features most significantly associated with tumor recurrence after LT in HCC patients were obtained by dimensionality reduction. Finally, the Rad-score of each patient was obtained by using the selected features and their weights with the following formula:

Rad-score = sigmoid [0.4908 × original_shape_MajorAxisLength (AP) + 0.2945 × wavelet-HHH_glszm_

Table 1 The demographic and clinicopathologic characteristics of the patients

Variable	Total (n=139)	Training cohort (n=97)	Validation cohort (n=42)	P
Age, years, mean ± SD	50.34±9.06	51.10±9.19	48.57±8.61	0.13
Sex, n (%)				0.42
Female	11 (7.91)	6 (6.19)	5 (11.90)	
Male	128 (92.09)	91 (93.81)	37 (88.10)	
HBsAg, n (%)				0.43
Negative	18 (12.95)	14 (14.43)	4 (9.52)	
Positive	121 (87.05)	83 (85.57)	38 (90.48)	
Child-Pugh classification, n (%)				0.83
A	61 (43.88)	42 (43.30)	19 (45.24)	
B	78 (56.12)	55 (56.70)	23 (54.76)	
AFP, ng/mL, n (%)				0.57
<200	98 (70.5)	67 (69.07)	31 (73.81)	
≥200	41 (29.5)	30 (30.93)	11 (26.19)	
ALP, U/L, n (%)				0.64
<135	92 (66.19)	63 (64.95)	29 (69.05)	
≥135	47 (33.81)	34 (35.05)	13 (30.95)	
Largest tumor size, cm, n (%)				0.28
<5	79 (56.83)	58 (59.79)	21 (50.00)	
≥5	60 (43.17)	39 (40.21)	21 (50.00)	
Tumor number, n (%)				0.85
Single	48 (34.53)	33 (34.02)	15 (35.71)	
Multiple	91 (65.47)	64 (65.98)	27 (64.29)	
Ki-67, n (%)				0.64
<10%	77 (55.4)	55 (56.70)	22 (52.38)	
≥10%	62 (44.6)	42 (43.30)	20 (47.62)	
Rad-score, mean ± SD	0.49±0.19	0.50±0.20	0.48±0.18	0.56
Milan criteria, n (%)				0.71
Within	40 (28.78)	27 (27.84)	13 (30.95)	
Beyond	99 (71.22)	70 (72.16)	29 (69.05)	
Hangzhou criteria, n (%)				0.43
Within	70 (50.36)	51 (52.58)	19 (45.24)	
Beyond	69 (49.64)	46 (47.42)	23 (54.76)	
DFS, months, mean ± SD	29.14±25.24	28.56±24.40	30.48±27.34	0.68
Recurrence, n (%)				0.96
No	60 (43.17)	42 (43.30)	18 (42.86)	
Yes	79 (56.83)	55 (56.70)	24 (57.14)	

SD, standard deviation; HBsAg, hepatitis B surface antigen; AFP, alpha-fetoprotein; ALP, alkaline phosphatase; Rad-score, radiomics score; DFS, disease-free survival.

Table 2 Univariate and multivariate Cox regression analyses for patients in the training cohort

Variables	Univariate analysis		Multivariable analysis	
	P	HR (95% CI)	P	HR (95% CI)
Age, years	0.97	1.00 (0.97–1.03)		
Sex (male *vs.* female)	0.30	1.71 (0.62–4.74)		
HBsAg (negative *vs.* positive)	0.70	0.86 (0.41–1.83)		
Child-Pugh class (A *vs.* B)	0.17	0.68 (0.40–1.18)		
AFP, ng/mL (≥200 *vs.* <200)	<0.001	4.12 (2.40–7.09)	0.02	2.05 (1.11–3.80)
ALP, U/L (≥135 *vs.* <135)	0.02	1.89 (1.10–3.22)	0.01	2.10 (1.16–3.81)
Largest tumor size, cm (<5 *vs.* ≥5)	0.002	0.43 (0.26–0.74)	0.85	0.94 (0.51–1.73)
Tumor number (single *vs.* multiple)	<0.001	0.16 (0.07–0.35)	<0.001	0.17 (0.07–0.42)
Ki-67, % (≥10 *vs.* <10)	<0.001	2.69 (1.57–4.62)	0.01	2.18 (1.21–3.92)
Rad-score (≥0.482 *vs.* <0.482)	<0.001	48.93 (11.72–204.32)	0.002	10.70 (2.39–47.99)

HR, hazard ratio; CI, confidence interval; HBsAg, hepatitis B surface antigen; AFP, alpha-fetoprotein; ALP, alkaline phosphatase; Rad-score, radiomics score.

ZoneEntropy (AP) – 0.0434 × original_shape_Sphericity (VP) + 0.1878 × wavelet-LHL_gldm_DependenceVariance (VP) + 0.0527 × wavelet-HHL_glszm_SmallAreaEmphasis (VP)]

In the training cohort, the Rad-score was normally distributed, so its median of 0.482 was used as the threshold value to categorize all patients into high-risk and low-risk groups. The DFS in the two groups was compared using Kaplan-Meier survival analysis in the training cohort and validation cohort (*Figure 2A*,*2B*). The 1-, 2-, and 3-year DFS rates in the low-risk group were 76.5%, 65.6%, and 62.5%, respectively. These figures were significantly higher than the high-risk group's 51.5%, 37.5%, and 31.3% in the training cohort, P<0.001. Additionally, the likelihood of recurrence in HCC patients was 2.71 times higher in the high-risk group than in the low-risk group. With significant differences in 1-, 2-, and 3-year DFS rates between the low-risk and high-risk groups (75.5%, 62.5%, 48.5% *vs.* 41.7%, 25.0%, 23.5%, P=0.023), radiomics features were confirmed in the validation cohort. Additionally, the likelihood of recurrence for HCC patients was 2.5 times higher in the high-risk group than in the low-risk group. There was an association between the Rad-score and DFS in both the training and validation cohorts. Therefore, the Rad-score was used to construct the RM.

CM, PM, and NM development

By Cox survival analysis, AFP, ALP, Ki-67, tumor number, and Rad-score were found to be independent predictors of DFS after LT in HCC patients (*Table 2*). Therefore, AFP and ALP were used to construct the CM, Ki-67, and tumor number were used to construct the PM, and the above five independent predictors were used to construct the NM (NM = CM + PM + RM) (*Figure 3*).

Performance comparison of CM, PM, RM, NM

In the training and validation cohorts, the AUCs of the four predictive models at 1, 2, and 3 years were first compared in predicting HCC recurrence using the Delong test as shown in *Figure 4* and *Table 3*, and the C-indexes of the four predictive models were compared as shown in *Table 3*. The final results revealed that the NM had the highest AUC and C-index in both the training cohort and the validation cohort. Consequently, for post-LT DFS in HCC patients, the NM had the best prediction performance among the four prediction models.

Consistency, clinical utility, and risk stratification capability evaluations of the NM

Figure 5A,*5B* show the training cohort and validation cohort calibration curves for the NM's prediction of DFS rates at 1, 2, and 3 years after LT in HCC patients, respectively, reflecting the high agreement between the NM's predicted DFS rates and actual DFS rates.

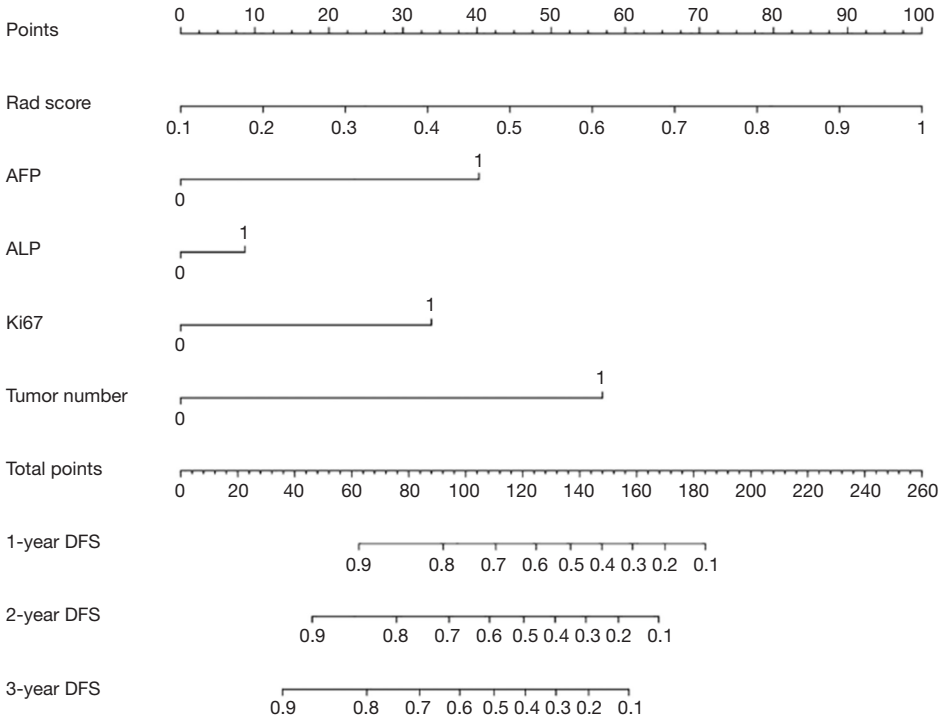

Figure 3 NM for the prediction of DFS status (AFP ≥200 ng/mL, ALP ≥135 U/L, Ki-67 ≥10%, multiple tumor numbers are defined as 1, and the Rad-score is entered according to the actual calculated value). AFP, alpha-fetoprotein; ALP, alkaline phosphatase; DFS, disease-free survival; NM, nomogram model.

Figure 6 displays the DCA curves for the four models. The NM excelled with the other three prediction models in terms of net clinical benefit in accurately predicting 1- and 2-year DFS with reasonable threshold probabilities.

To further explore the risk stratification ability of the NM, the total score of the NM for each patient was first calculated, and it was found that the total score conformed to a normal distribution in both the training cohort and the validation cohort. The obtained median of 0.573 was then used as the critical value to categorize the patients into low-risk or high-risk groups. As shown in *Figure 7A*,*7B*, Kaplan-Meier survival curves proved that the DFS of patients in the low-risk group was significantly prolonged (P<0.001), indicating that the NM had better risk stratification ability.

Discussion

In this study, we developed the NM for predicting DFS after LT in HCC patients. The training cohort and validation cohort C-indexes of the NM were 0.817 and 0.760, respectively. The calibration curves showed better predictive concordance between the training cohort and the validation cohort. Compared with CM, PM, and RM, the AUCs of NM were highest, indicating the NM's higher accuracy in predicting DFS; in the DCA curves, the NM predicted more clinical benefit of 1- and 2-year DFS after LT in HCC patients. In addition, the NM was able to risk-stratify patients, with a significant difference in DFS between the high-risk and low-risk groups. After LT in HCC patients, we were able to use NM to effectively predict patient DFS. This allows clinicians to start supplementary treatment before the occurrence of the high-risk period for recurrence, and it can also serve as a basis for warning patients to shorten their follow-up intervals promptly, improving their prognosis.

Predicting the patient's prognosis accurately has become crucial to individualized treatment and better patient outcomes as precision medicine has grown. ITH has been found to be common in numerous tumor types, and it is linked to metastasis and tumor progression as well as a poor prognosis (22). Nevertheless, the data on ITH derived from traditional clinical assessments are limited. CECT, as a

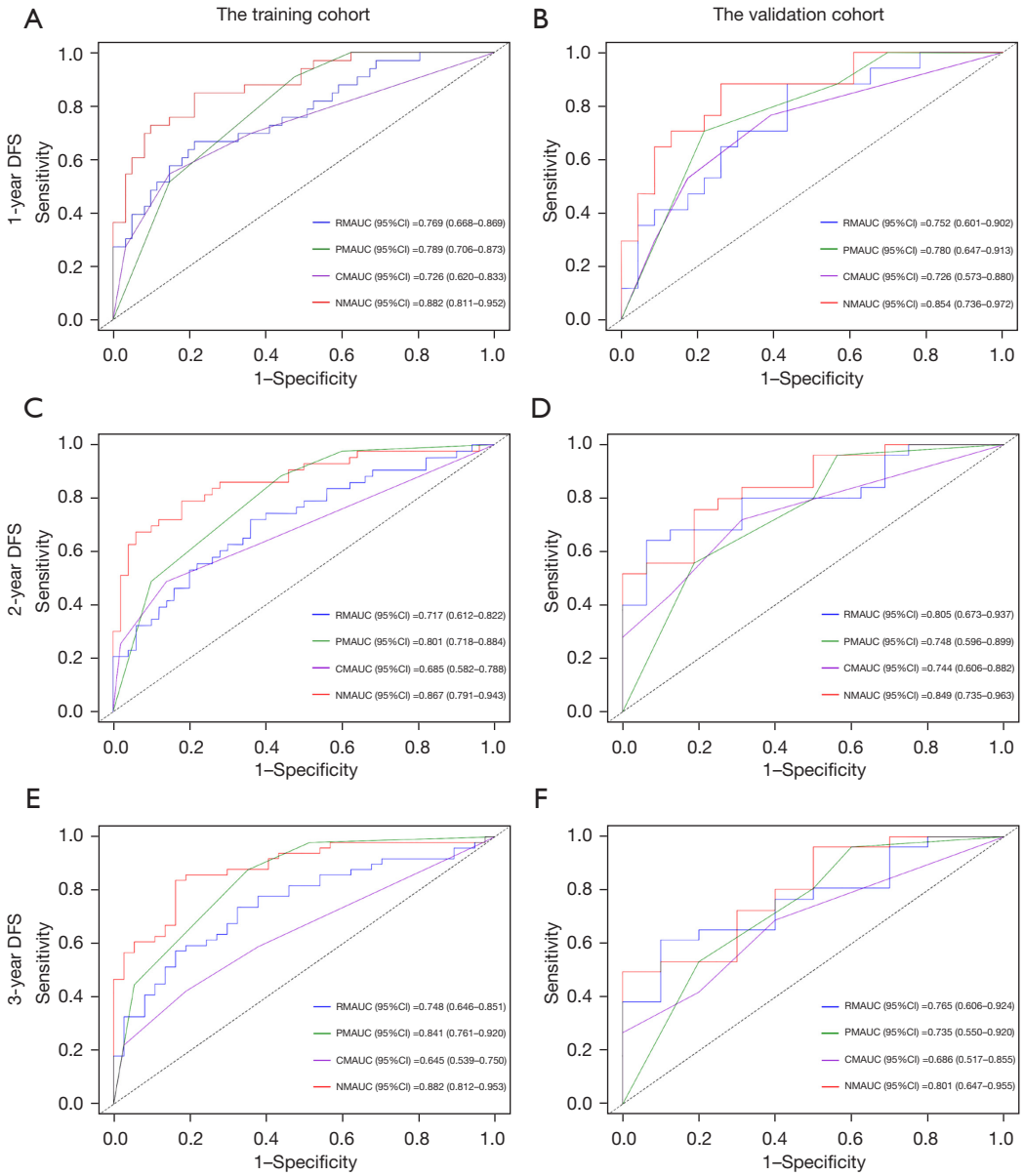

Figure 4 Time-ROC curves of the CM, PM, RM, and NM. AUC, area under the receiver operating characteristic curve; CM, clinical model; CI, confidence interval; DFS, disease-free survival; NM, nomogram model; PM, pathological model; ROC, receiver operating characteristic curve; RM, radiomics model.

standardized imaging modality, is widely used for diagnosis, staging, clinical decision-making, and monitoring of therapeutic responses in a variety of cancer types. Radiomics overcomes the constraints of conventional imaging and provides full information about ITH. Radiomics features have been demonstrated to have possible predictive importance in liver (23), lung (24), and breast cancers (25). The benefit of using radiomics is that it allows analysis of accessible CECT images. To forecast the prognosis of HCC patients, multiphase dynamic analysis is needed (26). Sufficient predictive information can be obtained from multiphase dynamic images to paint an exhaustive representation of ITH (26,27). Radiomics features extracted from AP- and VP-CECT images are closely related to the prognosis of HCC patients (26,28). Most of the previous radiomics studies (29-31), however, were not integrated

Table 3 The performance of the models in predicting recurrence of hepatocellular carcinoma after liver transplantation in the training and validation cohorts

Model	C-index (95% CI)		1-year AUC (95% CI)		2-year AUC (95% CI)		3-year AUC (95% CI)	
	Training cohort	Validation cohort	Training cohort	Validation cohort	Training cohort	Validation cohort	Training cohort	Validation cohort
CM	0.664 (0.586–0.742)	0.676 (0.579–0.772)	0.726 (0.620–0.833)	0.726 (0.573–0.880)	0.685 (0.582–0.788)	0.744 (0.606–0.882)	0.645 (0.539–0.750)	0.686 (0.517–0.855)
PM	0.737 (0.674–0.799)	0.691 (0.589–0.792)	0.789 (0.706–0.873)	0.780 (0.647–0.913)	0.801 (0.718–0.884)	0.748 (0.596–0.899)	0.841 (0.761–0.920)	0.735 (0.550–0.920)
RM	0.706 (0.635–0.778)	0.697 (0.607–0.786)	0.769 (0.668–0.869)	0.752 (0.601–0.902)	0.717 (0.612–0.822)	0.805 (0.673–0.937)	0.748 (0.646–0.851)	0.765 (0.606–0.924)
NM	0.817 (0.763–0.871)	0.760 (0.677–0.843)	0.882 (0.811–0.952)	0.854 (0.736–0.972)	0.867 (0.791–0.943)	0.849 (0.735–0.963)	0.882 (0.812–0.953)	0.801 (0.647–0.955)

CI, confidence interval; AUC, area under the receiver operating characteristic curve; CM, clinical model; PM, pathological model; RM, radiomics model; NM, nomogram model.

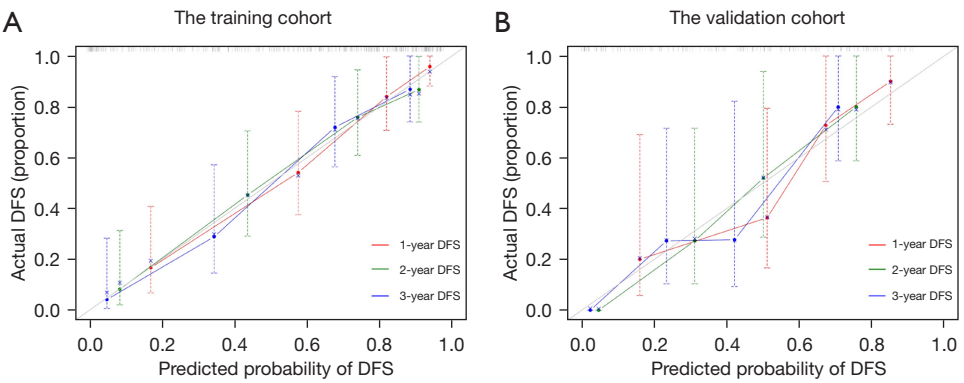

Figure 5 Calibration curves of the NM. DFS, disease-free survival; NM, nomogram model.

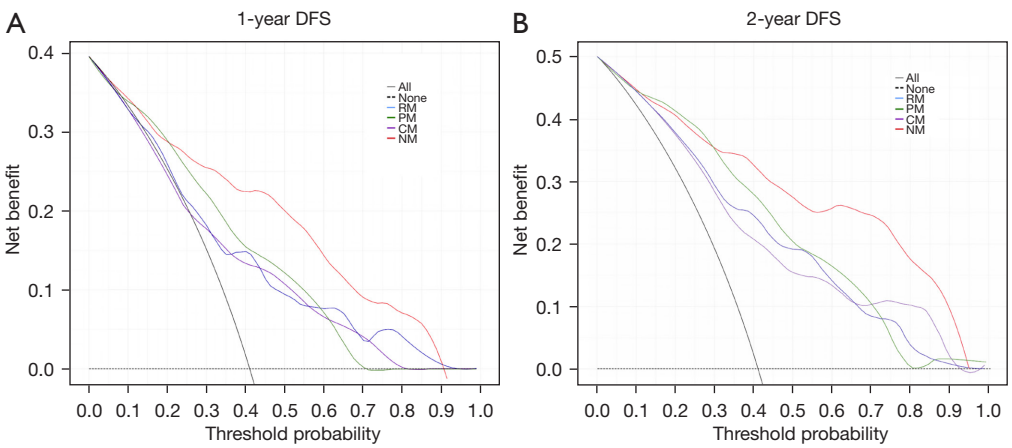

Figure 6 DCA for CM, PM, RM, and NM in all cohorts. CM, clinical model; DCA, decision curve analysis; DFS, disease-free survival; NM, nomogram model; PM, pathological model; RM, radiomics model.

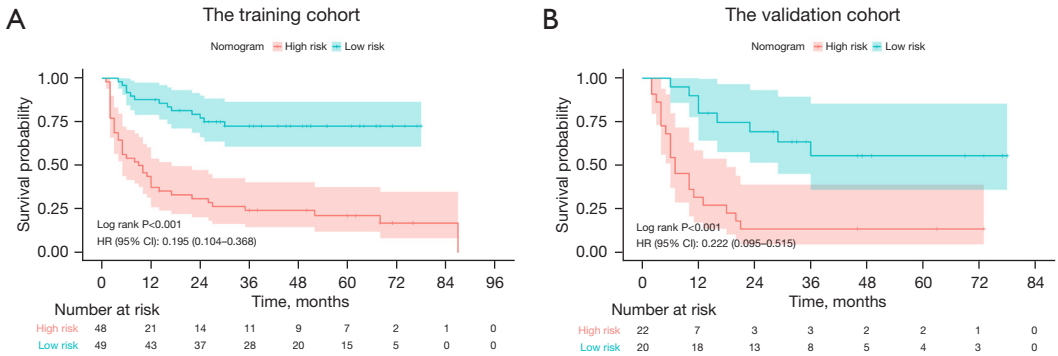

Figure 7 Estimated DFS of HCC patients after LT by NM (A,B). DFS, disease-free survival; HCC, hepatocellular carcinoma; LT, liver transplantation; NM, nomogram model; HR, hazard ratio; CI, confidence interval.

with the clinical features and pathological indicators of the patients. In contrast, in the present study, only the Rad-score was used as an important component of the NM and was calculated by obtaining five radiomics features from AP- and VP-CECT images associated with post-LT recurrence in HCC patients. Ultimately, the NM had a good predictive performance, which was not only a confirmation of previous studies but also an extremely important addition.

AFP was found to be an independent risk factor for postoperative survival, but it was not capable to predict prognosis in small HCCs (≤3 cm in diameter) (32). Another study showed that the ALP level was one of the most important independent predictors of recurrence and was even more important than AFP (33). AFP and ALP are routine blood tests for HCC patients that are not only easy to obtain but also relatively inexpensive. After LT, pathological examination revealing Ki-67 expression, tumor diameter and size, and other relevant pathologies are usually performed on the diseased liver. In conclusion, AFP, ALP, Ki-67, and tumor diameter and number may be independent predictors of prognosis in patients with HCC. However, in the aforementioned studies, it was often difficult to cope with AFP-negativity or small HCCs as independent prognostic predictors (34,35). In addition, more studies were performed to predict the expression of Ki-67 rather than using it as a prognostic independent predictor (13,21,36,37), whereas in this study, to accurately predict the prognosis of the patients in different aspects and to take full advantage of the available preoperative and postoperative data, AFP, ALP, Ki-67, and tumor numbers were all finally included in the NM as important prognostic independent predictors.

In a recent comparative study (38), it was reported that HCC patients with early recurrence after LT had significantly lower OS at 5 and 10 years than those with late recurrence. An improved ability to predict HCC recurrence would guide potential clinical adjuvant therapy, thereby improving the quality of long-term patient survival. Therefore, the endpoint of this study was DFS, not OS.

To our knowledge, this is the first NM based on CT radiomics to be used to predict DFS after LT in HCC patients, including AFP, ALP, and Ki-67. In some previous studies (21,36,37), radiomics was first used to predict Ki-67 expression in HCC patients and then indirectly to determine the prognosis of the patients. Previously, predictive models were also developed that were based on radiomics and were further constructed after combining clinical features or pathological indicators. To predict the prognosis of patients after radical surgery for HCC, Chong *et al.* (39) built a RM based on MRI imaging and included the pathological feature MVI. The validation cohort's mean AUC was 0.879 (95% CI: 0.820–0.938). Liu *et al.* (40) developed a RM based on CECT images and incorporated some clinical factors to predict OS after hepatectomy in patients with HCC, and the validation cohort had AUCs of 0.80, 0.81, and 0.78 for 1-, 2-, and 3-year OS, respectively. Therefore, our study was a direct use of postoperative Ki-67 expression in diseased livers, which, together with AFP, ALP, tumor number, and CT radiomics, was used to construct an NM for a multidimensional analysis of HCC patients, providing a more comprehensive tumor evaluation and a more effective DFS prediction. Compared with previous studies, NM could also enable risk stratification for HCC patients after LT and then be used to guide the follow-up and complementary treatment.

There are several limitations in this study. First, the primary weakness of this single-center retrospective analysis may have been the absence of data heterogeneity. As a

result, additional patients from other facilities are needed to confirm the clinical applicability and dependability of the NM. Second, alcohol, aflatoxin, hepatitis B virus (HBV), and hepatitis C virus (HCV) are generally recognized as multiple etiologic factors contributing to HCC. Different etiologic factors may lead to different outcomes in liver cancer. In our study, only one case of HBV, which presents the highest percentage of incidence, was investigated as being the main etiologic agent of HCC. Therefore, future studies are needed to validate the validity and accuracy of the NM in HCCs with different etiologies. Third, it is still unclear how biological behaviors and radiomics features relate to one another. Precision medicine is being developed, and rad-genomics, an emerging field now exploring the link between radiomics and genomics, is crucial. In future studies, we will need to combine genomics features associated with HCC prognosis to construct a more comprehensive integrated rad-genomics-based prediction model.

Conclusions

To summarize, this study fully utilized the preoperative clinical features, preoperative CT radiomics, and postoperative pathological indicators of patients to develop and validate a more precise NM that could guide adjuvant treatment and follow-up after LT and predict DFS in HCC patients.

Acknowledgments

Funding: None.

Footnote

Reporting Checklist: The authors have completed the TRIPOD reporting checklist. Available at https://jgo.amegroups.com/article/view/10.21037/jgo-24-347/rc

Data Sharing Statement: Available at https://jgo.amegroups.com/article/view/10.21037/jgo-24-347/dss

Peer Review File: Available at https://jgo.amegroups.com/article/view/10.21037/jgo-24-347/prf

Conflicts of Interest: All authors have completed the ICMJE uniform disclosure form (available at https://jgo.amegroups.com/article/view/10.21037/jgo-24-347/coif). The authors have no conflicts of interest to declare.

Ethical Statement: The authors are accountable for all aspects of the work in ensuring that questions related to the accuracy or integrity of any part of the work are appropriately investigated and resolved. The study was conducted in accordance with the Declaration of Helsinki (as revised in 2013). The study was approved by the Medical Ethics Review Committee of the Third Medical Center of Chinese People's Liberation Army (PLA) General Hospital (No.KY2024-016) and individual consent for this retrospective analysis was waived.

References

1. Forner A, Llovet JM, Bruix J. Hepatocellular carcinoma. Lancet 2012;379:1245-55.
2. Zhou J, Sun H, Wang Z, et al. Guidelines for the Diagnosis and Treatment of Hepatocellular Carcinoma (2019 Edition). Liver Cancer 2020;9:682-720.
3. Sung H, Ferlay J, Siegel RL, et al. Global Cancer Statistics 2020: GLOBOCAN Estimates of Incidence and Mortality Worldwide for 36 Cancers in 185 Countries. CA Cancer J Clin 2021;71:209-49.
4. Bray F, Ferlay J, Soerjomataram I, et al. Global cancer statistics 2018: GLOBOCAN estimates of incidence and mortality worldwide for 36 cancers in 185 countries. CA Cancer J Clin 2018;68:394-424.
5. Azoulay D, Audureau E, Bhangui P, et al. Living or Brain-dead Donor Liver Transplantation for Hepatocellular Carcinoma: A Multicenter, Western, Intent-to-treat Cohort Study. Ann Surg 2017;266:1035-44.
6. Sapisochin G, Goldaracena N, Astete S, et al. Benefit of Treating Hepatocellular Carcinoma Recurrence after Liver Transplantation and Analysis of Prognostic Factors for Survival in a Large Euro-American Series. Ann Surg Oncol 2015;22:2286-94.
7. Liu Q, Li J, Liu F, et al. A radiomics nomogram for the

prediction of overall survival in patients with hepatocellular carcinoma after hepatectomy. Cancer Imaging 2020;20:82.
8. Gupta S, Bent S, Kohlwes J. Test characteristics of alpha-fetoprotein for detecting hepatocellular carcinoma in patients with hepatitis C. A systematic review and critical analysis. Ann Intern Med 2003;139:46-50.
9. Li J, Cheng ZJ, Liu Y, et al. Serum thioredoxin is a diagnostic marker for hepatocellular carcinoma. Oncotarget 2015;6:9551-63.
10. Yeh CN, Chen MF, Lee WC, et al. Prognostic factors of hepatic resection for hepatocellular carcinoma with cirrhosis: univariate and multivariate analysis. J Surg Oncol 2002;81:195-202.
11. Gerdes J, Schwab U, Lemke H, et al. Production of a mouse monoclonal antibody reactive with a human nuclear antigen associated with cell proliferation. Int J Cancer 1983;31:13-20.
12. Gu Q, Feng Z, Liang Q, et al. Machine learning-based radiomics strategy for prediction of cell proliferation in non-small cell lung cancer. Eur J Radiol 2019;118:32-7.
13. Jiang T, Jiang W, Chang S, et al. Intratumoral analysis of digital breast tomosynthesis for predicting the Ki-67 level in breast cancer: A multi-center radiomics study. Med Phys 2022;49:219-30.
14. Cao Y, Ke R, Wang S, et al. DNA topoisomerase IIα and Ki67 are prognostic factors in patients with hepatocellular carcinoma. Oncol Lett 2017;13:4109-16.
15. Murakami K, Kasajima A, Kawagishi N, et al. Microvessel density in hepatocellular carcinoma: Prognostic significance and review of the previous published work. Hepatol Res 2015;45:1185-94.
16. Guzman G, Alagiozian-Angelova V, Layden-Almer JE, et al. p53, Ki-67, and serum alpha feto-protein as predictors of hepatocellular carcinoma recurrence in liver transplant patients. Mod Pathol 2005;18:1498-503.
17. Roberts LR, Sirlin CB, Zaiem F, et al. Imaging for the diagnosis of hepatocellular carcinoma: A systematic review and meta-analysis. Hepatology 2018;67:401-21.
18. Deng PZ, Zhao BG, Huang XH, et al. Preoperative contrast-enhanced computed tomography-based radiomics model for overall survival prediction in hepatocellular carcinoma. World J Gastroenterol 2022;28:4376-89.
19. Ortiz-Ramón R, Larroza A, Ruiz-España S, et al. Classifying brain metastases by their primary site of origin using a radiomics approach based on texture analysis: a feasibility study. Eur Radiol 2018;28:4514-23.
20. Jin X, Zheng X, Chen D, et al. Prediction of response after chemoradiation for esophageal cancer using a combination of dosimetry and CT radiomics. Eur Radiol 2019;29:6080-8.
21. Wu H, Han X, Wang Z, et al. Prediction of the Ki-67 marker index in hepatocellular carcinoma based on CT radiomics features. Phys Med Biol 2020;65:235048.
22. Sarobe P, Corrales F. Getting insights into hepatocellular carcinoma tumour heterogeneity by multiomics dissection. Gut 2019;68:1913-4.
23. Zheng BH, Liu LZ, Zhang ZZ, et al. Radiomics score: a potential prognostic imaging feature for postoperative survival of solitary HCC patients. BMC Cancer 2018;18:1148.
24. Huang Y, Liu Z, He L, et al. Radiomics Signature: A Potential Biomarker for the Prediction of Disease-Free Survival in Early-Stage (I or II) Non-Small Cell Lung Cancer. Radiology 2016;281:947-57.
25. Li H, Zhu Y, Burnside ES, et al. MR Imaging Radiomics Signatures for Predicting the Risk of Breast Cancer Recurrence as Given by Research Versions of MammaPrint, Oncotype DX, and PAM50 Gene Assays. Radiology 2016;281:382-91.
26. Kim S, Shin J, Kim DY, et al. Radiomics on Gadoxetic Acid-Enhanced Magnetic Resonance Imaging for Prediction of Postoperative Early and Late Recurrence of Single Hepatocellular Carcinoma. Clin Cancer Res 2019;25:3847-55.
27. Meng XP, Wang YC, Ju S, et al. Radiomics Analysis on Multiphase Contrast-Enhanced CT: A Survival Prediction Tool in Patients With Hepatocellular Carcinoma Undergoing Transarterial Chemoembolization. Front Oncol 2020;10:1196.
28. Hasdemir DB, Dávila LA, Schweitzer N, et al. Evaluation of CT vascularization patterns for survival prognosis in patients with hepatocellular carcinoma treated by conventional TACE. Diagn Interv Radiol 2017;23:217-22.
29. Zhou Y, He L, Huang Y, et al. CT-based radiomics signature: a potential biomarker for preoperative prediction of early recurrence in hepatocellular carcinoma. Abdom Radiol (NY) 2017;42:1695-704.
30. Shan QY, Hu HT, Feng ST, et al. CT-based peritumoral radiomics signatures to predict early recurrence in hepatocellular carcinoma after curative tumor resection or ablation. Cancer Imaging 2019;19:11.
31. Mao B, Zhang L, Ning P, et al. Preoperative prediction for pathological grade of hepatocellular carcinoma via machine learning-based radiomics. Eur Radiol 2020;30:6924-32.
32. Giannini EG, Marenco S, Borgonovo G, et al. Alpha-fetoprotein has no prognostic role in small hepatocellular

carcinoma identified during surveillance in compensated cirrhosis. Hepatology 2012;56:1371-9.
33. Yu MC, Chan KM, Lee CF, et al. Alkaline phosphatase: does it have a role in predicting hepatocellular carcinoma recurrence? J Gastrointest Surg 2011;15:1440-9.
34. Koch C, Bette T, Waidmann O, et al. AFP ratio predicts HCC recurrence after liver transplantation. PLoS One 2020;15:e0235576.
35. Özdemir F, Baskiran A. The Importance of AFP in Liver Transplantation for HCC. J Gastrointest Cancer 2020;51:1127-32.
36. Fan Y, Yu Y, Wang X, et al. Radiomic analysis of Gd-EOB-DTPA-enhanced MRI predicts Ki-67 expression in hepatocellular carcinoma. BMC Med Imaging 2021;21:100.
37. Liu Z, Yang S, Chen X, et al. Nomogram development and validation to predict Ki-67 expression of hepatocellular carcinoma derived from Gd-EOB-DTPA-enhanced MRI combined with T1 mapping. Front Oncol 2022;12:954445.
38. El-Domiaty N, Saliba F, Vibert E, et al. Early Versus Late Hepatocellular Carcinoma Recurrence After Transplantation: Predictive Factors, Patterns, and Long-term Outcome. Transplantation 2021;105:1778-90.
39. Chong HH, Yang L, Sheng RF, et al. Multi-scale and multi-parametric radiomics of gadoxetate disodium-enhanced MRI predicts microvascular invasion and outcome in patients with solitary hepatocellular carcinoma ≤ 5 cm. Eur Radiol 2021;31:4824-38.
40. Liu Y, Wei X, Zhang X, et al. CT radiomics combined with clinical variables for predicting the overall survival of hepatocellular carcinoma patients after hepatectomy. Transl Oncol 2022;26:101536.

Cite this article as: Xie H, Shi B, Fan J, Liu S, Ma Q, Dai J, Dong S, Liu Y, Meng H, Liu H, Yang Y, Mu X. A predictive model based on radiomics, clinical features, and pathologic indicators for disease-free survival after liver transplantation for hepatocellular carcinoma: a 7-year retrospective study. J Gastrointest Oncol 2024;15(5):2187-2200. doi: 10.21037/jgo-24-347

Supplementary

Table S1 CT parameters and the corresponding values

Parameter	Value
Tube voltage (KV)	120
Tube current	Auto
Detector collimation (mm)	64×0.625
Pitch of spiral	1.375
Matrix size	512×512
Slice interval (mm)	1.25
Slice thickness (mm)	1.25

https://dx.doi.org/10.21037/jgo-24-347